Chapter 8

OVERVIEW OF SOLAR FLARES

The Yohkoh Perspective

Hugh Hudson
Space Sciences Laboratory, UC, Berkeley CA USA 94720
hhudson@ssl.berkeley.edu

Lyndsay Fletcher
Dept. of Physics & Astronomy, University of Glasgow, Glasgow G12 8QQ, Scotland, U.K.
lyndsay@astro.gla.ac.uk

Josef I. Khan
Dept. of Physics & Astronomy, University of Glasgow, Glasgow G12 8QQ, Scotland, U.K.
jkhan@spd.aas.org

Takeo Kosugi
Institute for Space and Astronautical Sciences, Sagamihara, Kanagawa, Japan
kosugi@solar.isas.jaxa.jp

Abstract This chapter reviews the physics of solar flares, with special emphasis on the past decade. During this decade first *Yohkoh* and then TRACE have drastically improved our observational capabilities for flares, with contributions also from the essentially non-flare instrumentation on SOHO and of course the ground-based observatories. In this review we assess how these new observations have changed our understanding of the basic physics of flares and consider the implications of these results for future observations with FASR. The discussion emphasizes flaring loops, flare ejecta, particle acceleration, and microflares.

Keywords: Flares, X-rays, ejecta, corona

1. Introduction

The physics of solar flares seems too broad a subject to review adequately within the confines of a single chapter, so we have adopted an alternate strategy here. We pick several key topics and for each briefly review its history, its development in the *Yohkoh* era (mainly the decade of the 1990s), and its potential for development via future observations. We hope to have touched upon the most important new developments related to solar flares, and regret that space does not allow a complete description of any of them.

A solar flare is a sudden brightening in the solar atmosphere, typically spread across all atmospheric layers and involving substantial mass motions and particle acceleration. Brightening implies energy dissipation, and the consensus now holds that the energy for a flare had been stored magnetically in the corona prior to the event. This energy builds up relatively gradually as the result of deep-seated convective motions that deliver magnetic stress into the corona in the form of non-potential magnetic fields; the twist representing this non-potentiality may reside in an emerging flux system. Radio observations from the 1950s, and then X-ray and γ-ray observations from space from the 1960s, revealed that solar flares begin with high-energy processes. The key elements are accelerated particles, the "evaporation" of large masses of high-pressure plasma into coronal magnetic loops, and (frequently) magnetic eruptions as observed in a variety of wavelengths. While almost all of these components had been known prior to the launch of the *Yohkoh* observatory in August, 1991, the decade that followed saw great clarification of the observational situation.

The specific topics discussed here are **the flare concept**, **flare loops**, **particle acceleration**, **ejections** (including **global waves**), and **microflares**. We start with a brief review of new observational capabilities (*Yohkoh*, SOHO, and TRACE), and end with a discussion of how flare models and theories have changed. In this limited review we cannot cite the literature comprehensively, but we do try to give both early and modern references wherever possible. Finally we do not generally discuss FASR's capability, because other chapters cover this, but our choice of topics emphasizes areas where FASR will contribute in major ways. *Yohkoh* has made major contributions to identifying and understanding the wealth of radio observations of the solar corona.

2. New Observational Capabilities

2.1 *Yohkoh*

Yohkoh carried two imaging instruments, the Hard X-ray Telescope (HXT; 15–93 keV) and the Soft X-ray Telescope (SXT; $\sim$3–50Å), as well as two instruments for spectroscopy (WBS and BCS), as summarized in Table 8.1. The observations extended from September, 1991, to December, 2001.

The SXT used grazing-incidence mirrors and a CCD readout (Tsuneta *et al.* 1991), and thus was a second-generation instrument following the film readouts of the Skylab soft X-ray telescopes. The new instrument had lower scattered-light levels, better spectral selection, better off-axis angular resolution, and (most important) the CCD. The linearity and speed of this type of detector readily allowed movie representations of the data. This made motions easier to recognize, and small-scale motions turned out to be almost ubiquitous, as suggested by the Skylab data (Gerassimenko *et al.* 1974).

The HXT (Kosugi *et al.* 1991) followed the earlier hard X-ray imagers on the Solar Maximum Mission and Hinotori. Its innovations consisted of speed (large effective area), plus a four-channel spectral capability extending over ∼15–93 keV.

Table 8.1. Instruments on board *Yohkoh*[a]

Instrument	Type	Spectral range
HXT	Synthesis imaging	15–93 keV (4 channels)
SXT	Direct imaging	∼3–50Å (5 filters)
BCS	X-ray line spectroscopy	SXV, CaXIX, FeXXV, FeXXVI
WBS	Broad-band spectroscopy	∼3 keV–20 MeV

[a] Svestka & Uchida, 1991

2.2 SOHO and TRACE; other facilities

The Solar and Heliospheric Observatory (SOHO), launched in 1995, carries instruments not optimized for flare research, but which have produced copious new results on flares; TRACE, launched in 1998 (Handy *et al.* 1999) remedied the lack of time resolution for UV and EUV observations and has also produced extensive flare observations. RHESSI, launched in 2002 (Lin *et al.* 2002), unfortunately does not overlap with the *Yohkoh* observations. The other facilities contributing greatly to our understanding during the *Yohkoh* era have been for the most part ground-based observatories, including the radioheliographs at Nançay, Nobeyama, and Owens Valley, and the VLA.

3. The Flare Concept

A general definition of "solar flare" was given in the Introduction. In this section we discuss the current state of knowledge of the geometry and physics of a solar flare in order to introduce concepts and terminology. The following sections then discuss what we think are the most relevant outstanding issues related to future observations with FASR: magnetic loop structure, particle acceleration, ejection and magnetic-field restructuring, and microflares. In much

of the discussion we make use of the language of the "standard model" of a flare (or a CME), namely that of large-scale magnetic reconnection. In the *Yohkoh* literature this is often referred to as the CSHKP model (Carmichael-Sturrock-Hirayama-Kopp-Pneuman). (See Aschwanden, 2002; Priest & Forbes, 2002 for modern descriptions).

3.1 Confined and LDE flares

The Skylab data led to a two-element classification of solar flares into *confined* and *eruptive* categories (Pallavicini *et al.* 1977), and this classification appears to work well enough for the *Yohkoh* data as well (§ 6). The confined flares typically appear as small bright loops with little large-scale motion other than that attributed to evaporation flows along the loops; the eruptive flares tend to lead to long-decay events (LDEs; MacCombie & Rust, 1979) with an arcade of loops, and to be more strongly associated with coronal mass ejections (CMEs). In both cases one can have a full development of radiative signatures across the whole spectrum, in the extreme ranging from kilometer wavelengths to high-energy γ-radiation, plus the emission of energetic particles from the Sun.

As has been well-known from the classical Hα observations of solar flares, even powerful eruptive events can sometimes occur in essentially quiet regions or in active regions so feeble as not to support sunspots. Such events were observed with Skylab in soft X-rays, forming the extreme end of the LDE population, and in the *Yohkoh* era we often refer to these as "global restructurings." These events appear in soft X-ray images as giant arcades, sometimes extending more than one solar radius in length. They generally arise in filament channels, and the largest ones occur in the polar-crown filament regions. We identify them with two-ribbon structures analogous to those of eruptive flares but outside active regions, as observed in the chromosphere (Harvey *et al.* 1986).

3.2 Flares and CMEs

The relationships between flares and CMEs have excited extensive discussion and some controversy. See Cliver & Hudson (2002) for recent impressions of this subject. Briefly speaking, flare physics is best known through radiation signatures, and CMEs through motions of coronal material seen with a coronagraph or other coronal imager. The eruptive flares involve mass motions as well, and often the same structures (filaments) can be identified in both flares and CMEs. Flares occur more frequently than CMES; most of the powerful flares (GOES X-class) have closely-associated CMEs with comparable total energy, although a few do not. Similarly a few of the most spectacular CMEs have negligible flare effects in the low corona, most famously the event of 7 January 1997 (Webb *et al.* 1998). The flare/CME association involves high-energy

particle signatures well studied via coronal radio emission at metric and longer wavelengths (see Chapter 2) and by *in situ* observations in the heliosphere.

The flares/CME connection became controversial in the 1990s, when there were suggestions that CMEs directly caused flaring, leading to the confusing usage "post-eruption loops" as a synonym for "eruptive flare." The *Yohkoh* era has seen much more detailed study of the relationship between flare and CME processes, to the extent that we now do not know which causes which, if either. It may depend upon the type of event, since the data clearly show more than one kind of CME. While unquestionably signatures of a coming eruption (e.g., the activation and slow rise of a filament) may precede the main flare effects, the actual eruptions appear to go hand-in-hand with the flare's radiation effects (Hudson & Webb, 1997; Zarro *et al.* 1999). Zhang *et al.* (2002) have confirmed the close simultaneity of CME acceleration and flare brightening found originally from the *Yohkoh* observations of expanding loops and dimmings. We now recognize that CME acceleration may coincide well with the impulsive phase of its associated flare (Nitta & Akiyama, 1999; Zhang *et al.* 2002). But even with our superior new data it seems premature to decide on the direction of causality, and indeed the flare and CME processes may be too closely intertwined physically to make this a meaningful exercise (Hudson & Cliver, 2001; Zhang *et al.* 2001).

4. Flare Loops

The corona consists, we believe, of a volume-filling magnetic field populated by hot plasma (the corona) in an intermittent manner. From the Skylab era we have known that there is no such thing as a smooth background corona, and that magnetic loops define structures everywhere within the coronal volume. When a flare occurs, soft X-ray observations typically show the sudden formation of bright closed loops; this brightening results from the expansion of new hot plasma from below into already well-defined coronal structures (Figure 8.1). The footpoints of the flare loops first become bright across a wide spectral range, and then the whole loop appears in high-temperature observations. The cooling post-flare loops fade gradually with time as the gas pressure decreases and the excess mass eventually drains back out of the corona. In this gradual or decay phase of a flare there is a definite temporal relationship between density and temperature, as discovered in numerical simulations by Serio *et al.* (1991): $n_e^2 \propto T_e$ (Takahashi *et al.* 1996), where n_e, T_e are the electron density and temperature respectively.

A flare observed in soft X-rays consists mainly of one or more magnetic loops; in every event these include almost stationary loops that appear (footpoints first) and then fade with time. In the LDEs (Long Decay Events) this gradual phase (fading) may be protracted to the extent that energy input must continue, since

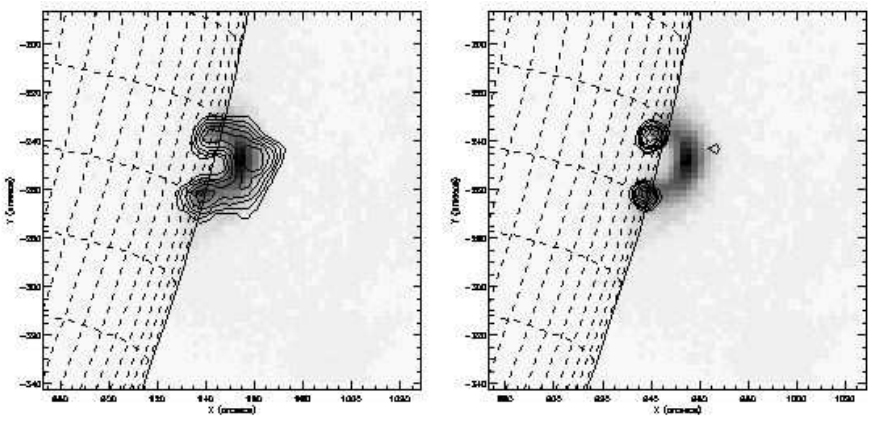

Figure 8.1. Soft and hard X-ray observations of the "Masuda flare", 13 January 1992, which nicely illustrates the coronal loop structure of a flare. Background image: soft X-rays (13 January 1992; reversed color table) from *Yohkoh* SXT. Contours: left, 15–23 keV; right, 23–33 keV from *Yohkoh* HXT. The contour above the soft X-ray loop shows the location of the Masuda source, and the contours at the ends of the soft X-ray loop show the hard X-ray footpoints. Although the contours tend to obscure them in this representation, the footpoints are also bright in soft X-rays.

the observed cooling time exceeds that expected theoretically (MacCombie & Rust, 1979; van Driel-Gesztelyi *et al.* 1997) over the lifetime of the loops. New loops must be appearing successively in the gradual phase, giving the (illusory) appearance of slow loop growth. This requirement helped to drive the development of the large-scale reconnection models, in which field lines opened during the flare process would then close, releasing magnetic energy to power the late phase of the flare.

In eruptive events some loops are violently ejected during the impulsive phase (Canfield *et al.* 1992; de Jager *et al.* 1984); this topic is deferred until § 6.

4.1 Footpoints, coronal spectroscopy, and evaporation

The footpoints of the flare loops often brighten impulsively (Figure 8.1). While this was known from earlier observations (Hoyng *et al.* 1981), the HXT data established the presence of this process for flares of GOES class C or above, and have allowed interesting time-resolved studies (Sakao *et al.* 1998; Masuda *et al.* 2001). Related impulsive brightenings take place all across the spectrum, including the "white light flare" phenomenon; the SXT observations clearly established this relationship (Hudson *et al.* 1992) and also show impulsive emission in soft X-rays as well (McTiernan *et al.* 1993; Hudson *et al.* 1994).

The footpoints show where chromospheric material is being heated, ionized, and channeled into the corona by the magnetic field (Neupert, 1968). The existence of such a phenomenon has long been inferred (more or less indirectly, in the absence of direct imaging) from the observation of EUV line shifts (e.g., Acton *et al.* 1982; Bentley *et al.* 1994).

The Bragg Crystal Spectrometer (BCS) on board *Yohkoh* continued the work of high-resolution X-ray spectroscopy of solar-flare plasmas (Culhane *et al.* 1991). *Yohkoh* lacked imaging spectroscopy, but SOHO instruments overcame this problem to a certain extent. Unfortunately they were not optimized for rapid time variability, and the SOHO spectroscopic instruments tended to avoid flare observations. However the evaporation flow has now also been imaged spectroscopically via SOHO (Czaykowska *et al.* 1999) even though a direct association with particle precipitation remains problematic (Czaykowska *et al.* 2001), at least in the late phase of an LDE.

The soft X-ray emission lines in flares typically show "non-thermal broadening"; the line widths exceed those expected from the thermal motions of the emitting ions. Determining the physical location of this signature (loop top or footpoints?) clearly would help us to understand flare evolution; if the non-thermal broadening results from small-scale turbulence, this might be identified with the site of the energy conversion. Without spatial resolution, *Yohkoh* efforts to localize the non-thermal broadening made use of limb occultation. Khan *et al.* (1995) studied a sequence of nearly homologous flares that were successively occulted by the limb, and found no substantial difference in non-thermal broadening. On the other hand Mariska *et al.* (1996) studied a different (but still small) sample of events, finding a tendency for the non-thermal broadening to be greater in the footpoints of the flare loops. Similarly the interpretation of the time-series development of non-thermal broadening (Alexander *et al.* 1998) is ambiguous. Alexander *et al.* (1998) and Harra *et al.* (2001) argue that the non-thermal broadening may appear *prior to* the impulsive hard X-rays, thus suggesting an early turbulent phase of energy release; Mariska & McTiernan (1999) and Ranns *et al.* (2001) on the other hand, find a closer relationship between the two signatures. These results are therefore ambiguous, but there is hope — Solar-B will have much better EUV imaging spectroscopy and should overlap with FASR.

4.2 Arcades

In many flares an elongated arcade of loops develops, probably never more spectacularly than in the "Bastille Day flare" of 2000 (Figure 8.2). These constitute one of the two categories of flare noted by Pallavicini *et al.* (1977), namely the compact loop flares and the eruptive flares, and this categorization appears to have a counterpart in the morphology of solar energetic particles (SEPs) ob-

served in the heliosphere (e.g., Reames, 1999). The loop and footpoint behavior of these two types of flare do not separate into any kind of bimodal distribution, since a compact flare loop has two footpoints equivalent to short ribbons. Bimodal behavior is seen more strongly in the SEP events—"impulsive" and "gradual" SEP events do occur, with the former associated more strongly with impulsive flares and the latter with CMEs (Reames, 1999).

The arcade morphology extends beyond the eruptive flares and into the domain of filament eruptions ("spotless flares") from the quiet corona (Harvey *et al.* 1986). More properly these might be called "quiescent filament-channel eruptions," since the role of the filament itself in the flare dynamics remains unclear (note though that Low, 2001, emphasizes the importance of the filament mass as an anchor for a flux rope that otherwise might rise via buoyancy). See Engvold (1994) for a description of filament channels. *Yohkoh*, EIT (the EUV Imaging Telescope), and TRACE (the Transition Region and Coronal Explorer) have observed many such arcade events, which may appear in GOES non-imaging X-ray data as long-decay events (LDEs)—or they may not; they are cooler and fainter than active-region events and frequently cannot be detected in whole-Sun X-ray data above the background, even if their X-ray images are striking. We suggest that similar physics, including the non-thermal aspects (e.g., Dennis & Zarro, 1993), extends through this category of flare as well as through the active-region events.

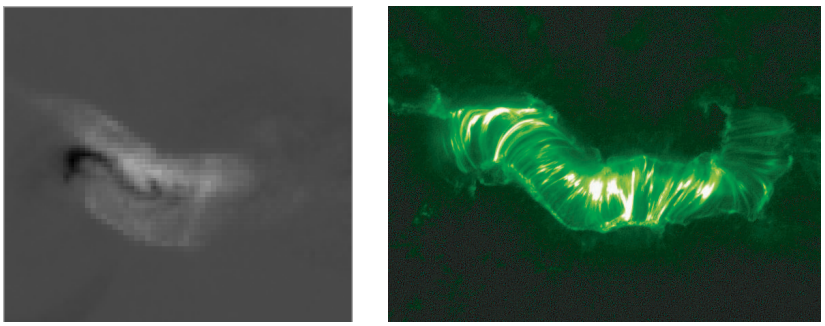

Figure 8.2. Yohkoh SXT difference image (left) and TRACE image (right) of the arcade flare of 14 July 2000 ("Bastille Day flare"), not to scale. The SXT difference images shows (as black) the pre-flare sigmoid, and (as white) the flare arcade. The TRACE image shows the full development of the large arcade, at lower temperatures.

The SXT observations of arcades revealed something not obvious in the EUV images: cusp-shaped structures, as shown in Figure 8.3. Because these resemble the general geometry of large-scale reconnection (and also the geometry of coronal streamers in particular) this observation immediately supported flare models involving reconnection (possibly, from the streamer analogy, between

field lines which have been opened; see Hiei *et al.*, 1993). Further evidence came from (i) the temperature structure observed by SXT in certain flares which suggested the pattern of slow shocks in the Petschek regime (Tsuneta, 1996*a*; Tsuneta, 1996*b*), and (ii) the presence of shrinkage within the cusp described by Hiei *et al.* 1997—it is this "dipolarization" of newly closed loops that actually converts the stored magnetic energy into kinetic energy (Svestka *et al.* 1987; Forbes & Acton, 1996).

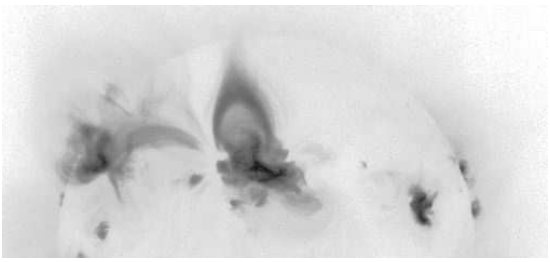

Figure 8.3. A beautiful cusp (following an X-class flare of 7 June 2000), as observed by SXT. This image shows the northern hemisphere of the Sun, and the scale can be judged from the limb.

In the latter half of the *Yohkoh* observations, as a result of improvements in the observing program, observations of a velocity fields around the arcade began to be noticed, as expected from the dimming signatures (§ 6.2). Yokoyama *et al.* (2001), for example, reported horizontal inward flows in a cusp geometry towards the apparent reconnection point. This observation made use of both EIT and SXT data, showing the temperature structure clearly, and an estimate of the inflow speed put it at on the order of 10^{-3} times the Alfvén speed.

While an inflow consistent with coronal reconnection has been reported only for the single event of Yokoyama *et al.* 2001, outflows (downward, towards the arcade) also consistent with the standard reconnection model have been detected many times by *Yohkoh* (McKenzie, 2000) and now by TRACE as well (Gallagher *et al.* 2002). These flows are known as a "Supra-Arcade Downflows" or SAD events. The first observations (McKenzie & Hudson, 1999) showed dark intrusions streaming down in between a spiky structure extending above the late-phase arcade (Švestka *et al.* 1998); such spikes form in a fraction of the arcade events and appear to map to individual loops of the arcade below. The downward velocities are much smaller than the inferred Alfvén speed, and usually smaller than the free-fall speed as well (McKenzie, 2000). The intrusions are voids (Innes *et al.* 2003) and occur in the impulsive phase, in association with hard X-ray bursts (Asai *et al.* 2004), as well as the gradual phase. This downward velocity field should be distinguished from that of the well-known "coronal rain," which occurs in the legs of an arcade as it cools. The

logical interpretation of the SADs would be in terms of reconnection ouflow jets, but several aspects of the observations remain puzzling (Why a spiky arcade? Why sub-Alfvénic downflow speeds? Why do voids appear in the flow?)

Figure 8.4. Left, soft X-ray observations of a spiky arcade event. The spikes extend above the NE limb to heights on the order of one solar radius; such events exhibit the "SAD" phenomenon described in the text.

4.2.1 "Sigmoids" and filament cavities. The association of S-shaped coronal soft X-ray features with eruptivity is a well-established, if not one-to-one, relationship (Sterling & Hudson, 1997; Canfield *et al.* 1999; Gibson *et al.* 2002). Figure 8.2 shows the disappearance of a sigmoid during the eruption of the Bastille Day 2000 flare. This "sigmoid-to-arcade" development is a characteristic pattern for such events (Sterling *et al.* 2000), with the simple interpretation that the sigmoid structure represents magnetic twist associated with field-aligned coronal current flow. Hagyard *et al.* (1984) had already found such regions to have enhanced flare probability. The sigmoid features probably consist of elongated flux ropes analogous to filament cavities (Engvold, 1994), which often appear as stable features of the quiet corona and which may have enormous spatial scales.

4.3 Loop-loop interactions

The SXT images of flares typically show multiple loops to be involved. In many cases *three* footpoints appear, showing two loops possibly interacting within one of them. This morphology was known from the Solar Maximum Mission (Machado *et al.* 1988) and from VLA observations, but was greatly extended with *Yohkoh* and Nobeyama observations (Hanaoka, 1997; Nishio *et al.* 1997). In such cases flaring in a primary compact loop sometimes appears to trigger a response in a larger-scale loop, and the configuration is often referred

to as a "loop-loop interaction." Such a geometry could also explain flares with apparently over-bright footpoints (e.g., Farnik *et al.* 1997), by hypothesizing that such a footpoint actually would consist of an unresolved bipolar loop structure. Although an analysis of loop-loop behavior can be made by assuming that the loops are discrete entities (Melrose, 1997), the common assumption is that the coronal magnetic field fills the entire volume, so that bright loops (in the low-β limit) may not really be distinct structures. It should be noted that cases of independent loop brightenings in flares also occur, with no apparent physical contact between the loops.

5. Particle Acceleration

Non-thermal particles play a fundamental role in solar flares and in CMEs. We can detect them directly in the heliosphere or remotely via their radiation signatures in various wavelength ranges. Hard X-rays from solar flares show the presence of energetic (semi-relativistic) electrons, accelerated by an as yet unidentified acceleration mechanism that operates in the impulsive phase of the flare. The significance of these observations follows from the large energy inferred to be present in the non-thermal electrons of the impulsive phase (Kane & Donnelly, 1971).

Imaging observations in the hard X-ray range ($>$10 keV) only began with the SMM and *Hinotori* spacecraft in the 1980s, and then only over a limited energy range. This imaging showed that fairly short (10^9 cm scale) magnetic loops could be the site of energy release even for some of the most powerful flares; these loops revealed their presence by double footpoint sources (Hoyng *et al.* 1981). In the footpoint region of a flaring loop, virtually every observable wavelength may show an impulsive emission component—cm-wave radio, white light, EUV, and soft X-rays as well as hard X-rays. Thus the phenomenon occurring in these regions must be highly non-thermal, consistent with the precipitation of the impulsive-phase energetic electrons from the corona in the form of directed beams.

5.1 Footpoint sources

The hard X-ray imager HXT on *Yohkoh* has greatly expanded our knowledge of the non-thermal particle populations in solar flares. In particular the images showed two footpoints in the majority of the many flares observed (Sakao, 1994), as illustrated in Figure 8.1. In other cases HXT only showed a single brightening, which could be interpreted as unresolved footpoints; in other cases more than two footpoints appeared. In most cases the soft X-ray images from SXT showed coronal loop structures connecting pairs of footpoints.

Sakao (1994) noted a tendency towards footpoint asymmetry, in the sense that the brighter footpoint of a conjugate pair tended to have the weaker photospheric

magnetic field as inferred from a magnetogram. This would be consistent with the magnetic mirror force restricting the electron propagation. More interestingly still, Sakao *et al.* (1998) found that the footpoints moved during the flare development, but not always in the direction (greater separation) expected from the standard reconnection model. This has opened an active field of research, in which the footpoint motions are interpreted in terms of their coronal connectivity (Somov & Kosugi, 1997; Fletcher & Hudson, 2001; Saba *et al.* 2001; Qiu *et al.* 2002; Somov *et al.* 2002). The observations in principle help in understanding not only the geometry of the magnetic restructuring causing the flare, but also its energetics since the non-thermal electrons carry such a large fraction of the total flare energy.

A ubiquitous "soft-hard-soft" pattern of spectral evolution (Parks & Winckler, 1969; Fletcher & Hudson, 2002) appears in the hard X-ray footpoint sources. There exists a theoretical description (Benz, 1977; Brown & Loran, 1985) based upon stochastic acceleration. Theories of impulsive-phase particle acceleration involving large-scale shock waves (Tsuneta & Naito, 1998) or acceleration actually in the reconnection region (Litvinenko, 2000) need to be shown consistent with this soft-hard-soft pattern.

5.2 Coronal sources

The *Yohkoh* soft X-ray observations show us the active behavior of all domains in the solar corona, and so the X-ray counterparts of the metric burst classification (types I through V) have all been identified. The results are clearest for the type II and type III bursts, as described elsewhere in this Chapter. Furthermore significant progress has been made in our understanding of the highly complex decimetric band, in particular the drifting pulsating sources (Kliem *et al.* 2000; Khan *et al.* 2002),

The "Masuda flare" phenomenon (Masuda *et al.* 1995) has had a substantial impact on our thinking about the physical mechanisms at work in solar flares. Briefly this refers to the presence of a hard X-ray source in the corona *above* the soft X-ray loops, visible during the impulsive phase of a flare as illustrated in Figure 8.1. The only feasible explanation for this phenomenon appears to be the presence of a sufficient target density in the emitting region (Fletcher, 1995; Wheatland & Melrose, 1995; Conway *et al.* 1998), in order that the inefficient thin-target bremsstrahlung process would be detectable. The need for high density can be mitigated by trapping (Fletcher & Martens, 1998), but this depends upon the unknown field geometry as well as on the acceleration mechanism. The standard reconnection models envision low-field regions (actually nulls in 2D models) which could serve as particle traps. The Masuda source occurs during the impulsive phase of a flare but appears to be unusual, in that surveys (Petrosian *et al.* 2002; Aschwanden, 2002) only revealed a handful of such

Masuda events among *Yohkoh*'s many flares. The prototype flare of January 13, 1992 (Figure 8.1) appears to have a high trapping efficiency (Aschwanden *et al.* 1999), which could be consistent with the time scale needed for the evaporation of sufficient material to form a dense bremsstrahlung target. Metcalf & Alexander (1999) have carried out a detailed analysis of the target density requirement in view of the spectral evolution in the Masuda source.

Upon its discovery the Masuda source was immediately interpreted in terms of the standard reconnection model (Masuda *et al.* 1995) involving a fast-mode MHD shock terminating the reconnection outflow. The hard X-ray source could arise in particle acceleration either at the shock itself via the Fermi mechanism, with trapping by the paired slow-mode shock structures present in the standard (2D) reconnection model (Tsuneta & Naito, 1998). This attractive idea has the added advantage that the particle acceleration takes place not at the point of reconnection, which may have a low density (the "number problem"; see Brown & Melrose, 1977), but in a closed loop structure that may already contain electrons or else gain additional electrons via the mechanism of chromospheric evaporation driven by the overall process. A stochastic acceleration model in a similar geometry (Larosa *et al.* 1996; Jakimiec *et al.* 1998) could also be consistent with the presence of energy conversion above the loop top.

In addition to the Masuda sources, closely related to the impulsive phase and to the flare loops themselves, there are other coronal hard X-ray sources more closely associated with eruption and CME development (Cliver *et al.* 1986 and references therein). To observe coronal hard X-ray sources with good sensitivity, it is best to study flares for which the bright footpoint sources are occulted (e.g., Tomczak, 2001). A recent *Yohkoh* example has been discussed by Sato (2001), who found good evidence for the trapping of non-thermal electrons in coronal loops. Hudson *et al.* (2001) also found a moving source from an over-the-limb flare on 18 April 2001. The hard X-ray source emerged from behind the limb in the form of a compact structure identifiable with a microwave source, and moved outwards at $\sim 10^3$ km s^{-1}.

5.3 Energetic ions

The energetic ion component (>1 MeV) of a solar flare, as revealed by its γ-ray line emission spectrum, may contain energy rivaling that of the impulsive-phase electrons and therefore of the entire flare process (Ramaty *et al.* 1995). *Yohkoh* confirmed the existence of two types of solar γ-ray bursts (Yoshimori *et al.* 1999), namely the normal events and the so-called "electron-rich" events. We expect substantial progress in γ-ray line spectroscopy from RHESSI (the Reuven Ramaty High-Energy Solar Spectroscopic Imager, launched in February 2002; see Lin *et al.* 2002).

6. Ejections

Flares originally were called "eruptions" by Hale, and we know now that this was apt terminology: an explosive restructuring of the coronal magnetic field often plays a key role in the physical development of a flare. Almost invariably, for the most powerful flares, this involves loop ejections, global wave generation, and the occurrence of a coronal mass ejection (CME). De La Beaujardière *et al.* (1995) and Green *et al.* (2002) have shown, however, that even major flares sometimes consist of "confined eruptions" that have no significant counterparts in the upper corona.

6.1 Parallel and perpendicular flows

Movie representations of the images often show motions both perpendicular and parallel to the inferred field direction. *Yohkoh* observations in particular immediately revealed parallel flows in the form of X-ray jets, previously unknown, often with apparent velocities on the order of 10^3 km s^{-1} (Shibata *et al.* 1992; Strong *et al.* 1992). These jets are highly-collimated plasma flows emerging from the vicinity of flaring loops (microflares; see § 7), often found in the leading-polarity region of a sunspot group (Shimojo *et al.* 1998). They also apparently mark the locations of channels for certain type III radio bursts (Aurass *et al.* 1994; Kundu *et al.* 1995).

The perpendicular motions (restructurings) occur in strong association with CMEs (Nitta & Akiyama, 1999), but also at lower speeds in expanding active regions (Uchida *et al.* 1992). Flares, especially major ones, frequently exhibit high-speed ejections (Hudson *et al.* 1996; Ohyama & Shibata, 1998; Innes *et al.* 2001). It is worth emphasizing that *non-radial* motions may characterize the early development of a flare ejection; this is often the appearance from *Yohkoh* images, although one cannot be sure because of the geometrical projection effects, but it can be demonstrated with full 3D reconstructions using high-resolution spectroscopic imaging (e.g., Penn, 2000).

6.2 Dimming

Dimming at soft X-ray and EUV wavelengths has become a prominent signature of coronal mass ejections, analogous to the "coronal depletions" seen in white light (Hansen *et al.* 1974). Because they have broad temperature response, both the white-light and X-ray decreases suggest a simple explanation: the dimmed material has been released to expand into the solar wind. We can distinguish four types of dimming (Hudson & Webb, 1997), all of which closely match the increase of flare brightening (Table 8.2) in temporal development.

From the original observations it was clear that the dimming time scale was inconsistent with cooling time scales, and hence must involve expansion of the

Table 8.2. Soft X-ray coronal dimming

Type	Prototype	Reference
Transient coronal hole	October 23, 1997	Rust, 1983
Diffuse	February 21, 1992	Hudson *et al.* 1995
Loop expansion	November 13, 1994	Nitta & Akiyama, 1999
Disappearing TIL[a]	May 6, 1998	Khan & Hudson, 2000

[a] Transequatorial interconnecting loop system

field (Hudson *et al.* 1996); in some cases this expansion appears to be arrested (de La Beaujardière *et al.* 1995; Green *et al.* 2002), but normally it involves the opening of active-region magnetic field lines into the interplanetary medium as a part of a CME. The SXT data show unambiguously that the temporal pattern of the dimming reflects that of the flare brightening, a result significant for discussions of flare/CME relationships (§ 3.2).

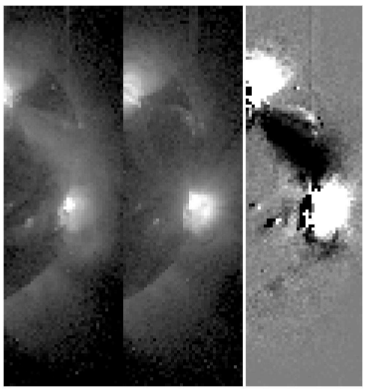

Figure 8.5. Disappearing trans-equatorial interconnecting loop (TIL) associated with the blast wave and CME of the flare of May 6, 1998 (Khan & Hudson, 2000). The left two panels show the W limb of the Sun before and after the disappearance; the right panel shows the difference at higher image contrast; the dark outline of the TIL represents dimming.

The trans-equatorial interconnecting loops (TILs) link active regions, or their near vicinities, across the solar equator (e.g., Svestka *et al.* 1977, Pevtsov, 2000). These TILs tend to have greater visibility in soft X-rays than in the lower-temperature EUV observations from EIT (as do the sigmoids; see §4). This points to the existence of a heating mechanism that may differ from that responsible for bright loops in active regions, which have small spatial scales, short time scales, and originate in strong-field regions. Note that filament channels, which also contain long field lines, tend to be cool and dark in soft

X-rays. In a striking observation Khan & Hudson (2000) found that such a loop structure may suddenly disappear (Figure 8.5). The event of 6 May 1998 (see also § 6.3) was the first of a set of three nearly homologous disappearances. Khan & Hudson, 2000 found that the timing suggested a disruption of the TIL by the flare blast wave; the TIL morphology closely agreed with the initial appearance of the CME as viewed by the LASCO coronagraphs.

6.3 Global waves

Prior to the 1990s, we knew of the existence of global coronal shock waves (analogous to supernova shocks) via their Moreton wave and meter-wave type II radio signatures. The obvious prediction for *Yohkoh* was there: SXT could observe the solar corona directly in its soft X-ray emission, and therefore the slow-mode MHD shock responsible for a type II burst (see Uchida, 1968), because it was compressive, should produce a bright ripple visible in a flare movie sequence.

In fact it required almost a decade before such sources were clearly identified (Khan & Aurass, 2002; Narukage *et al.* 2002; Hudson *et al.* 2003). The reasons for this delay are complex, but in the meanwhile the EIT instrument on SOHO had made clear detections of related coronal waves (Moses *et al.* 1997, Thompson *et al.* 1998). Although considerable debate has accompanied the development of consensus on this point (e.g., Cliver & Hudson, 2002), we now feel sure that two types of large-scale waves occur. The immediate blast wave begins in the magnetic-restructuring disturbance at the onset of the flare impulsive phase; as it moves outward it develops into a fast-mode MHD shock wave and "ignites" as a type II burst at metric wavelengths (e.g., Vršnak, 2001). At the same time the CME, if one occurs, moves outward and drives an interplanetary shock ahead of it. This wave, unlike the blast wave, can continue as long as the CME propagates supersonically; when it arrives at the Earth it makes a clear signature in the geomagnetic field (the "storm sudden commencement").

The observations of the 6 May 1998 wave event in soft X-rays (Figure 8.6) allowed us to study its development within 10^9 cm of the flare core. In fact, the wave did not appear to originate at the core loops of the flare, but rather from a radiant point significantly displaced from it. This tends to rule out a "pressure pulse" explanation for the wave formation, and instead points to the field restructuring itself as the direct cause—not an implausible situation in what is believed to be plasma at low β, where gas pressure itself should have a negligible effect.

The "EIT wave" phenomenon (Thompson *et al.* 1998) actually now appears to comprise both blast waves and restructurings (Delannée, 2000). The fastest of the waves have a strong correlation with flares and type II bursts and thus

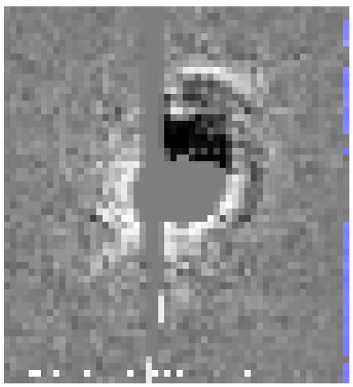

Figure 8.6. Soft X-ray signature of 6 May 1998 wave. The image shows a difference image at a 40 s spacing from the SXT AlMg filter with $10''$ pixels, at a time several minutes after the initiation time of the event as determined by its radiant (Hudson *et al.* 2003). The neutral gray area, including the vertical spike, show regions of CCD saturation; field-of-view $\sim 10'$.

agree with Uchida's unifying theory of type IIs and Moreton waves (Biesecker *et al.* 2002).

7. Microflares and Nanoflares

"Microflares," in the sense of flare-like events with total energies on the order of 10^{26} ergs, were already evident in the GOES data, a B1 event being about 10^{-4} the energy of a GOES X10 event. Theoretical insight (Parker, 1988) and hard X-ray observations (Lin *et al.* 1984) suggested that tiny non-thermal events might play a major energetic role in active regions or even the entire corona. But to do so required "nanoflares," even tinier events whose numbers and frequency might merge into the appearance of a continuous heating of the coronal plasma. Hudson (1991) pointed out that the microflare observations (from various sources) in fact showed occurrence-frequency distributions of total flare energy W for which $N(W) \sim W^{-\alpha}$, with $\alpha < 2$. The energy in such distributions is dominated by large events, not small ones, and so the nanoflare phenomenon needed to be found in events not strictly resembling the flares and microflares. The SXT observations provided the first good imaging X-ray data for this purpose with adequate temporal sampling.

The *Yohkoh* soft X-ray imaging immediately revealed the locations of the smallest GOES events, which for the most part turned out to be flare-like brightenings in active regions (Shimizu *et al.* 1992). These then were the soft X-ray counterparts of the hard X-ray microflares originally observed by Lin *et al.* 1984. Detailed studies in soft X-rays (Shimizu *et al.* 1994) and at other wavelengths (White *et al.* 1995; Gary *et al.* 1997; Shimizu *et al.* 2002) have subsequently

provided little evidence to suggest the presence of any substantially different physics represented; hence "microflare" seems a reasonable name for a flare-like event on such a scale. The microflares occur in a power-law distribution with total energy in a manner consistent with flare observations (e.g., Hudson, 1991; as shown in Figure 8.7 they span the energy range down to about 10^{27} ergs before a roll-over attributable to selection effects for the smaller events.

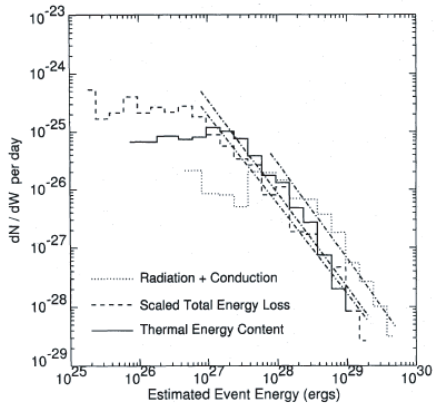

Figure 8.7. Energy distributions for microflares observed with the *Yohkoh* SXT (Shimizu, 1995), incorporating plausible physical models to scale the total energy (necessary because soft X-rays only contain a small portion, roughly 1/15, of the total event energy). The flattening of the distribution for small event energies represents detection threshold.

Despite these results some controversy has continued to simmer, as EUV observations of these microflares and of still smaller "micro-events" in the quiet Sun (e.g., Berghmans *et al.* 1998; Parnell & Jupp, 2000; Aschwanden & Charbonneau, 2002; Benz & Krucker, 2002) became available. Partly this may have stemmed from the more complex morphologies of the EUV observations but the ambiguities of the modeling needed to interpret the observations physically also seems to have contributed to the continuing discussion. Can the microflares themselves be taken as a signature of coronal heating? The flatness of the distribution function suggests not (Hudson, 1991), but the conversion from any observable signature to the total energy of an event requires extensive model-dependent adjustments and we may not know how to do it correctly. To answer this question one must deal correctly with sampling bias—the equivalent of the cosmologist's "Malmquist bias" (Aschwanden & Charbonneau, 2002). Our current knowledge of the energies and distributions of flare-like events, at present, suggests that they have little to do with the heating of the general corona.

8. Evolution of Flare Theories and Models

Theories of flares and CMEs, often indistinguishable in their essence, have generally followed the line of the standard large-scale reconnection (CSHKP) model. This involves either an ideal MHD catastrophe or a dissipative process that opens the magnetic field of an active region, allowing it to re-form with energy release into the cusped arcade structure made familiar with *Yohkoh* images (Priest & Forbes, 2002). Theoretical treatments of these phenomena based upon MHD will always have trouble with self-consistency, however, because of the strong effects of particle acceleration. Recent work has emphasized the 3D nature of the phenomena, the topology of the coronal magnetic field in terms of separatrices or "quasi-separatrix structures" that separate domains of connectivity, the role of statistical sub-processes working in a self-organizing manner, and the physics of magnetic helicity.

At the simplest level of this theoretical work, there is now convincing evidence, in the late phases of eruptive flares, for the large-scale reconnection picture presented by CSHKP models. Current thinking distinguishes between eruptions occurring from "tether-cutting" reconnection (Moore & Labonte, 1980) which can occur in an essentially bipolar magnetic configuration, and eruptions requiring more complex connectivity (e.g., the "breakout" model of Antiochos, 1998). One apparent problem of all such magnetic models is the need to circumvent the "Aly conjecture," which suggests that the open configuration of the field has greater energy than the closed configuration. Opening the field therefore would absorb energy, rather than releasing it as observed during a flare. How to avoid this problem remains unclear, but there are suggestions that the problem does not exist for partial eruptions of the field (Sturrock *et al.* 2001), or that the conjecture itself may simply be wrong (Choe & Cheng, 2002).

The idea that magnetic energy stored slowly in the corona can be released suddenly to power a flare or CME is almost unanimous. Unfortunately we have only sketchy knowledge of the coronal magnetic field because of the extreme difficulty of direct observations and because extrapolation from the photospheric magnetograms has fundamental uncertainties. Thus it has recently become interesting to make use of the flare observations to define both the connectivity and also infer something about the site of energy storage and release. In particular Aschwanden (2002) has developed a comprehensive view of flare structure including the use of accelerated particles both as tracers in the lower atmosphere and also as time-of-flight guides to the middle corona where energy may be stored.

9. Conclusions

Even though many of the *Yohkoh* observations were merely nice refinements of earlier discoveries, many also have had "breakthrough" quality. This decade-long flood of wonderful observations has taught us a great deal, and from the data archive many research workers around the world are still finding new things. With RHESSI to fill in some of the gaps and to extend our knowledge in the key area of non-thermal particle behavior, the epoch beginning in 1991 will no doubt be recognized as the most important yet for our understanding of flare physics. From the theoretical point of view, we are now beginning to study the 3D geometry of the flare catastrophe, and it is very interesting—FASR will help greatly on this score, because of its capability to make direct coronal magnetic-field measure (see Chapter 12). This suggests the possible development of coronal loop seismology (see Roberts, 2000 and references therein) leading to inference of coronal properties such as the magnetic field intensity (Nakariakov & Ofman, 2001).

Acknowledgments

NASA supported the work of HSH under NAS 5-98033, and he thanks the Astronomy and Astrophysics Group of the University of Glasgow for hospitality during the writing of this Chapter.

References

Acton, L. W., Leibacher, J. W., Canfield, R. C., Gunkler, T. A., Hudson, H. S., & Kiplinger, A. L. 1982, ApJ, 263, 409

Alexander, D., Harra-Murnion, L. K., Khan, J. I., & Matthews, S. A. 1998, ApJ, 494, L235

Antiochos, S. K. 1998, ApJ, 502, L181

Asai, A., Yokoyama, T., Shimojo, M., & Shibata, K. 2004, ApJ, 605, L77

Aschwanden, M. J. 2002, Space Sci. Rev., 101, Nos. 1-2, Kluwer Academic Publishers, Dordrecht.

Aschwanden, M. J. & Charbonneau, P. 2002, ApJ, 566, L59

Aschwanden, M. J., Fletcher, L., Sakao, T., Kosugi, T., & Hudson, H. 1999, ApJ, 517, 977

Aurass, H., Klein, K.-L., & Martens, P. C. H. 1994, Solar Phys, 155, 203

Bentley, R. D., Doschek, G. A., Simnett, G. M., Rilee, M. L., Mariska, J. T., Culhane, J. L., Kosugi, T., & Watanabe, T. 1994, ApJ, 421, L55

Benz, A. O. 1977, ApJ, 211, 270

Benz, A. O. & Krucker, S. . 2002, ApJ, 568, 413

Berghmans, D., Clette, F., & Moses, D. 1998, A&A, 336, 1039

Biesecker, D. A., Myers, D. C., Thompson, B. J., Hammer, D. M., & Vourlidas, A. 2002, ApJ, 569, 1009
Brown, J. C. & Loran, J. M. 1985, MNRAS, 212, 245
Brown, J. C. & Melrose, D. B. 1977, Solar Phys, 52, 117
Canfield, R. C., Hudson, H. S., Leka, K. D., Mickey, D. L., Metcalf, T. R., Wuelser, J., Acton, L. W., Strong, K. T., Kosugi, T., Sakao, T., Tsuneta, S., Culhane, J. L., Phillips, A., & Fludra, A. 1992, PASJ, 44, L111
Canfield, R. C., Hudson, H. S., & McKenzie, D. E. 1999, GRL, 26, 627
Choe, G. S. & Cheng, C. Z. 2002, ApJ, 574, L179
Cliver, E. W., Dennis, B. R., Kiplinger, A. L., Kane, S. R., Neidig, D. F., Sheeley, N. R., & Koomen, M. J. 1986, ApJ, 305, 920
Cliver, E. W. & Hudson, H. S. 2002, J. Atm. & Terr. Phys., 64, 231
Conway, A. J., MacKinnon, A. L., Brown, J. C., & McArthur, G. 1998, A&A, 331, 1103
Culhane, J. L., Bentley, R. D., Hiei, E., Watanabe, T., Doschek, G. A., Brown, C. M., Cruise, A. M., Lang, J., Ogawara, Y., & Uchida, Y. 1991, Solar Phys, 136, 89
Czaykowska, A., Alexander, D., & De Pontieu, B. 2001, ApJ, 552, 849
Czaykowska, A., de Pontieu, B., Alexander, D., & Rank, G. 1999, ApJ, 521, L75
de Jager, C., Boelee, A., & Rust, D. M. 1984, Solar Phys, 92, 245
de La Beaujardière, J.-F., Canfield, R. C., Hudson, H. S., Wulser, J.-P., Acton, L., Kosugi, T., & Masuda, S. 1995, ApJ, 440, 386
Delannée, C. 2000, ApJ, 545, 512
Dennis, B. R. & Zarro, D. M. 1993, Solar Phys, 146, 177
Engvold, O. 1994, IAU Colloq. 144, Solar Coronal Structures, p297
Farnik, F., Hudson, H., & Watanabe, T. 1997, A&A, 324, 433
Fletcher, L. 1995, A&A, 303, L9
Fletcher, L. & Hudson, H. S. 2001, Solar Phys, 204, 69
Fletcher, L. & Hudson, H. S. 2002, Solar Phys, 210, 307
Fletcher, L. & Martens, P. C. H. 1998, ApJ, 505, 418
Forbes, T. G. & Acton, L. W. 1996, ApJ, 459, 330
Gallagher, P. T., Dennis, B. R., Krucker, S., A., S. R., & Tolbert, A. K. 2002, Solar Phys, 210, 341
Gary, D. E., Hartl, M. D., & Shimizu, T. 1997, ApJ, 477, 958
Gerassimenko, M., Golub, L., Kahler, S., & Petrasso, R. 1974, Coronal Disturbances, IAU Symp. 57, 501
Gibson, S. E., Fletcher, L., Del Zanna, G., Pike, C. D., Mason, H. E., Mandrini, C. H., Démoulin, P., Gilbert, H., Burkepile, J., Holzer, T., Alexander, D., Liu, Y., Nitta, N., Qiu, J., Schmieder, B., & Thompson, B. J. 2002, ApJ, 574, 1021

Green, L. M., Matthews, S. A., van Driel-Gesztelyi, L., Harra, L. K., & Culhane, J. L. 2002, Solar Phys, 205, 325
Hagyard, M. J., Teuber, D., West, E. A., & Smith, J. B. 1984, Solar Phys, 91, 115
Hanaoka, Y. 1997, Solar Phys, 173, 319
Handy, B. N. *et al.* 1999, Solar Phys, 187, 229
Hansen, R. T., Garcia, C. J., Hansen, S. F., & Yasukawa, E. 1974, PASP, 86, 500
Harra, L. K., Matthews, S. A., & Culhane, J. L. 2001, ApJ, 549, L245
Harvey, K. L., Sheeley, N. R., & Harvey, J. W. 1986, Solar-Terrestrial Predictions, (P.A. Simon *et al.* eds.), 2, 198
Hiei, E., Hundhausen, A. J., and Sime, D. G. 1993, GRL, 20, 2785
Hiei, E., Hundhausen, A. J., & Burkepile, J. 1997, ASP Conf. Ser. 111, Magnetic Reconnection in the Solar Atmosphere, 383
Hoyng, P., Duijveman, A., Machado, M. E., Rust, D. M., Svestka, Z., Boelee, A., de Jager, C., Frost, K. T., Lafleur, H., Simnett, G. M., van Beek, H. F., & Woodgate, B. E. 1981, ApJ, 246, L155
Hudson, H. S. 1991, Solar Phys, 133, 357
Hudson, H. S., Acton, L. W., Alexander, D., Freeland, S. L., Lemen, J. R., & Harvey, K. L. 1995, Solar Wind Conference, p58
Hudson, H. S., Acton, L. W., & Freeland, S. L. 1996, ApJ, 470, 629
Hudson, H. S., Acton, L. W., Hirayama, T., & Uchida, Y. 1992, PASJ, 44, L77
Hudson, H. S. & Cliver, E. W. 2001, JGR, 106, 25199
Hudson, H. S., Khan, J. I., Lemen, J. R., Nitta, N. V., & Uchida, Y. 2003, Solar Phys, 212, 121
Hudson, H. S., Kosugi, T., Nitta, N. V., & Shimojo, M. 2001, ApJ, 561, L211
Hudson, H. S., Strong, K. T., Dennis, B. R., Zarro, D., Inda, M., Kosugi, T., & Sakao, T. 1994, ApJ, 422, L25
Hudson, H. S. & Webb, D. F. 1997, Geophysical Monographs, 99, 27.
Innes, D. E., Curdt, W., Schwenn, R., Solanki, S., Stenborg, G., & McKenzie, D. E. 2001, ApJ, 549, L249
Innes, D. E., McKenzie, D. E., & Wang, T. 2003, Solar Phys, 217, 247
Jakimiec, J., Tomczak, M., Falewicz, R., Phillips, K. J. H., & Fludra, A. 1998, A&A, 334, 1112
Kane, S. R. & Donnelly, R. F. 1971, ApJ, 164, 151
Khan, J. I. & Aurass, H. 2002, A&A, 383, 1018
Khan, J. I., Harra-Murnion, L. K., Hudson, H. S., Lemen, J. R., & Sterling, A. C. 1995, ApJ, 452, L153
Khan, J. I. & Hudson, H. S. 2000, GRL, 27, 1083
Khan, J. I., Vilmer, N., Saint-Hilaire, P., and Benz, A. O. 2002, A&A, 388, 363
Kliem, B., Karlický, M., & Benz, A. O. 2000, A&A, 360, 715

Kosugi, T., Masuda, S., Makishima, K., Inda, M., Murakami, T., Dotani, T., Ogawara, Y., Sakao, T., Kai, K., & Nakajima, H. 1991, Solar Phys, 136, 17
Kundu, M. R., Raulin, J. P., Nitta, N., Hudson, H. S., Shimojo, M., Shibata, K., & Raoult, A. 1995, ApJ, 447, L135
Larosa, T. N., Moore, R. L., Miller, J. A., & Shore, S. N. 1996, ApJ, 467, 454
Lin, R. P., Schwartz, R. A., Kane, S. R., Pelling, R. M., & Hurley, K. C. 1984, ApJ, 283, 421
Lin et al., R. P. *et al.* 2002, Solar Phys, 210, 3
Litvinenko, Y. E. 2000, Solar Phys, 194, 327
Low, B. C. 2001, JGR, 106, 25141
MacCombie, W. J. & Rust, D. M. 1979, Solar Phys, 61, 69
Machado, M. E., Moore, R. L., Hernandez, A. M., Rovira, M. G., Hagyard, M. J., & Smith, J. B. 1988, ApJ, 326, 425
Mariska, J. T. & McTiernan, J. M. 1999, ApJ, 514, 484
Mariska, J. T., Sakao, T., & Bentley, R. D. 1996, ApJ, 459, 815
Masuda, S., Kosugi, T., Hara, H., Sakao, T., Shibata, K., & Tsuneta, S. 1995, PASJ, 47, 677
Masuda, S., Kosugi, T., & Hudson, H. S. 2001, Solar Phys, 204, 55
McKenzie, D. E. 2000, Solar Phys, 195, 381
McKenzie, D. E. & Hudson, H. S. 1999, ApJ, 519, L93
McTiernan, J. M., Kane, S. R., Loran, J. M., Lemen, J. R., Acton, L. W., Hara, H., Tsuneta, S., & Kosugi, T. 1993, ApJ, 416, L91
Melrose, D. B. 1997, ApJ, 486, 521
Metcalf, T. R. & Alexander, D. 1999, ApJ, 522, 1108
Moore, R. L. & Labonte, B. J. 1980, IAU Symposium 91, 207
Moses, D., *et al.* 1997, Solar Phys, 175, 571
Nakariakov, V. M. & Ofman, L. 2001, A&A, 372, L53
Narukage, N., Hudson, H. S., Morimoto, T., Akiyama, S., Kitai, R., Kurokawa, H., & Shibata, K. 2002, ApJ, 572, L109
Neupert, W. M. 1968, ApJ, 153, L59
Nishio, M., Yaji, K., Kosugi, T., Nakajima, H., & Sakurai, T. 1997, ApJ, 489, 976
Nitta, N. & Akiyama, S. 1999, ApJ, 525, L57
Ohyama, M. & Shibata, K. 1998, ApJ, 499, 934
Pallavicini, R., Serio, S., & Vaiana, G. S. 1977, ApJ, 216, 108
Parker, E. N. 1988, ApJ, 330, 474
Parks, G. K. & Winckler, J. R. 1969, ApJ, 155, L117
Parnell, C. E. & Jupp, P. E. 2000, ApJ, 529, 554
Penn, M. J. 2000, Solar Phys, 197, 313
Petrosian, V., Donaghy, T. Q., & McTiernan, J. M. 2002, ApJ, 569, 459
Pevtsov, A. A. 2000, ApJ, 531, 553
Priest, E. R. & Forbes, T. G. 2002, Astron. Ap. Revs., 10, 313

Qiu, J., Lee, J., Gary, D. E., & Wang, H. 2002, ApJ, 565, 1335
Ramaty, R., Mandzhavidze, N., Kozlovsky, B., & Murphy, R. J. 1995, ApJ, 455, L193
Ranns, N. D. R., Harra, L. K., Matthews, S. A., & Culhane, J. L. 2001, A&A, 379, 616
Reames, D. V. 1999, Space Sci. Rev., 90, 413
Roberts, B. 2000, Solar Phys, 193, 139
Rust, D. M. 1983, Space Sci. Rev., 34, 21
Saba, J. L. R., Gaeng, T., & Tarbell, T. D. 2001, *Yohkoh* 10th Ann. Meeting., 96
Sakao, T. 1994, Ph.D. Thesis, U. Tokyo
Sakao, T., Kosugi, T., & Masuda, S. 1998, ASSL Vol. 229, 273
Sato, J. 2001, ApJ, 558, L137
Serio, S., Reale, F., Jakimiec, J., Sylwester, B., & Sylwester, J. 1991, A&A, 241, 197
Shibata, K., Ishido, Y., Acton, L. W., Strong, K. T., Hirayama, T., Uchida, Y., McAllister, A. H., Matsumoto, R., Tsuneta, S., Shimizu, T., Hara, H., Sakurai, T., Ichimoto, K., Nishino, Y., & Ogawara, Y. 1992, PASJ, 44, L173
Shimizu, T. 1995, PASJ, 47, 251
Shimizu, T., Shine, R. A., Title, A. M., Tarbell, T. D., & Frank, Z. 2002, ApJ, 574, 1074
Shimizu, T., Tsuneta, S., Acton, L. W., Lemen, J. R., Ogawara, Y., & Uchida, Y. 1994, ApJ, 422, 906
Shimizu, T., Tsuneta, S., Acton, L. W., Lemen, J. R., & Uchida, Y. 1992, PASJ, 44, L147
Shimojo, M., Shibata, K., & Harvey, K. L. 1998, Solar Phys, 178, 379
Somov, B. V. & Kosugi, T. 1997, ApJ, 485, 859
Somov, B. V., Kosugi, T., Hudson, H. S., Sakao, T., & Masuda, S. 2002, ApJ, 579, 863
Sterling, A. C. & Hudson, H. S. 1997, ApJ, 491, L55
Sterling, A. C., Hudson, H. S., Thompson, B. J., & Zarro, D. M. 2000, ApJ, 532, 628
Strong, K. T., Harvey, K., Hirayama, T., Nitta, N., Shimizu, T., & Tsuneta, S. 1992, PASJ, 44, L161
Sturrock, P. A., Weber, M., Wheatland, M. S., & Wolfson, R. 2001, ApJ, 548, 492
Svestka, Z., Krieger, A. S., Chase, R. C., & Howard, R. 1977, Solar Phys, 52, 69
Svestka, Z. & Uchida, Y. 1991, The YOHKOH (Solar-A) Mission (Dordrecht: Kluwer Academic Publishers)
Svestka, Z. F., Fontenla, J. M., Machado, M. E., Martin, S. F., & Neidig, D. F. 1987, Solar Phys, 108, 237

Takahashi, M., Watanabe, T., Sakai, J., Sakao, T., Kosugi, T., Sakurai, T., Enome, S., Hudson, H. S., Hashimoto, S., & Nitta, N. 1996, PASJ, 48, 857

Thompson, B. J., Plunkett, S. P., Gurman, J. B., Newmark, J. S., St. Cyr, O. C., & Michels, D. J. 1998, GRL, 25, 2465

Tomczak, M. 2001, A&A, 366, 294

Tsuneta, S. 1996*a*, ApJ, 456, 840

Tsuneta, S. 1996*b*, ApJ, 464, 1055

Tsuneta, S., Acton, L., Bruner, M., Lemen, J., Brown, W., Caravalho, R., Catura, R., Freeland, S., Jurcevich, B., & Owens, J. 1991, Solar Phys, 136, 37

Tsuneta, S. & Naito, T. 1998, ApJ, 495, L67

Uchida, Y. 1968, Solar Phys, 4, 30

Uchida, Y., McAllister, A., Strong, K. T., Ogawara, Y., Shimizu, T., Matsumoto, R., & Hudson, H. S. 1992, PASJ, 44, L155

Švestka, Z. . K., Fárník, F. ., Hudson, H. S., & Hick, P. 1998, Solar Phys, 182, 179

van Driel-Gesztelyi, L., Wiik, J. E., Schmieder, B., Tarbell, T., Kitai, R., Funakoshi, Y., & Anwar, B. 1997, Solar Phys, 174, 151

Vršnak, B. 2001, JGR, 106, 25249

Webb, D. F., Cliver, E. W., Gopalswamy, N., Hudson, H. S., & St. Cyr, O. C. 1998, GRL, 25, 2469

Wheatland, M. S. & Melrose, D. B. 1995, Solar Phys, 158, 283

White, S. M., Kundu, M. R., Shimizu, T., Shibasaki, K., & Enome, S. 1995, ApJ, 450, 435

Yokoyama, T., Akita, K., Morimoto, T., Inoue, K., & Newmark, J. 2001, ApJ, 546, L69

Yoshimori, M., Shiozawa, A., & Suga, K. 1999, Proc. Nobeyama Symposium, Kiyosato, Japan, (T. S. Bastian, N. Gopalswamy & K. Shibasaki, eds.), NRO Report 479, 353

Zarro, D. M., Sterling, A. C., Thompson, B. J., Hudson, H. S., & Nitta, N. 1999, ApJ, 520, L139

Zhang, J., Dere, K. P., Howard, R. A., Kundu, M. R., & White, S. M. 2001, ApJ, 559, 452

Zhang, M., Golub, L., DeLuca, E., & Burkepile, J. 2002, ApJ, 574, L97